RSC Advances

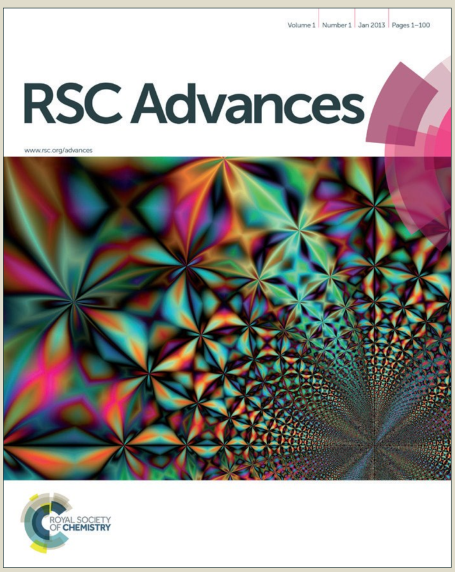

Non-destructively sensing pork's quality indicators using near infrared multispectral imaging technique

Qiping Huang, Huanhuan Li, Jiewen Zhao, Gengping Huang, Quansheng Chen*

School of Food and Biological Engineering, Jiangsu University, Zhenjiang 212013, P.R. China

∗ Corresponding author. Tel.: +86-511-88790318. Fax: +86-511-88780201.
E-mail: qschen@ujs.edu.cn (QS Chen)

Abstract

Near infrared multispectral imaging system (MSI) based on three wavebands namely 1280nm, 1440nm and 1660nm was developed for non-destructively sensing pork's tenderness and Water Holding Capacity (WHC) of pork. Multispectral images were acquired for pork samples, and the real tenderness (Warner-Bratzler shear force, WBSF) and WHC (cook loss, CL) of these samples were simultaneously determined using traditional destructive methods. The gray level co-occurrence matrix (GLCM) was used for extraction of characteristic variables from multispectral images. Next, ant colony optimization combined with back propagation artificial neural network, namely ACO-BPANN, was used for modeling, which achieved good performance compared with the other two commonly used algorithms. The correlations coefficient and the root mean square error in the prediction set were achieved as follows: $Rp = 0.8451$ and $RMSEP = 0.9087$ for WBSF; $Rp = 0.9116$ and $RMSEP = 1.5129$ for CL. This work adequately demonstrated that the MSI technique has a high potential usage in non-destructively sensing pork's quality attributes combined with an appropriate algorithm, thus facilitating simple and fast way of identification and classification of meat in a.

Keywords: pork meat; Warner-Bratzler Shear Force (WBSF); Cook Loss (CL); Multispectral Imaging (MSI); Ant Colony Optimization (ACO)

1.Introduction

The quality of raw meat is usually influenced by a variety of factors which include animal (breed, sex, age), environmental (feeding, transporting and slaughtering condition), and processing (storing time, temperature condition).[1] It is well known that all the meat supplied to the markets must undergo quality control in order to guarantee consumer safety, and some consumers are willing to pay higher prices for meat products with an additional guarantee of quality.[2]

There are many quality traits such as pH, color, texture, water holding capacity, tenderness, and freshness, and so on for assessing the quality of meat.[2-4] Among them, tenderness and Water Holding Capacity (WHC) are regarded as the most important parameters in the assessment of eating quality of meat.[5] Nowadays, tenderness and WHC of pork meat are commonly measured by destructive physicochemical means. As one of important attributes, tenderness is correlated with many factors, such as species and the age of the animal at slaughter time. Usually, Warner-Bratzler Shear Force (WBSF) is seen as a reference index in evaluation of pork's tenderness. Determination of pork tenderness is performed by texture meters equipped with Warner-Bratzler, Kramer or compression devices.[6] WHC, defined as the ability of muscle to retain water or resist water loss, is an important reference index used to evaluate pork's eating quality.[7] In the past few years, WHC of pork was measured using different procedures such as fluid loss, drip loss, thaw loss and cook loss. However, these traditional methods are impracticability because they are time consuming, laborious and destructive amidst other constraints. Therefore, it is of great significance to explore a more rapid, efficient and nondestructive method for pork quality determination.

In the past decade, many researchers reported that some non-destructive techniques were successfully used for detection of pork's quality. Among the non-destructive techniques, Near-infrared (NIR) spectroscopy is a widely used and increasingly growing technique due to its rapidity, simplicity, and its ability to measure chemical properties or characteristics of food products.[8-10] In our previous studies, NIR spectroscopy was implemented to evaluate pork freshness and tenderness.[1, 11] Nevertheless, the NIR technique merely captures the single-point information of the sample, which is not sufficient to indicate the whole quality of the samples. Furthermore, the change of pork quality is often accompanied with the changes from the external attributes (color, texture, etc.) and internal attributes (chemical compositions, tissue structure, etc.).[12] Therefore, it is the key to seek a technology for obtaining outside and inside information. Recently, owing to its integration of traditional imaging and spectroscopy, hyperspectral imaging (HSI) technology was widely used for detection of food quality.[13-17] However, the exorbitant price and the huge data obtained during HSI slows down the detection speed, and thus rendering it only a laboratory set-up which can hardly serve the purpose of real-time usage.[18] To satisfy the need of production in food industry, developing a low-cost system is especially important for monitoring of food quality and safety.

Multispectral imaging (MSI) is an emerging platform technique with advantages of rapid, chemical-free, non-destructive and so on compared with conventional analytical methods. In contrast to the conventional NIR spectroscopy, it integrates traditional imaging and spectroscopy to attain both spatial and spectral information from objects. Although MSI technique only obtains a few images at a discrete spectral region by positioning a band-pass filter in front of a monochrome camera, the optimum waveband filters are found by HSI technique to develop a MSI system for practical usage. Compared with the HSI technique, the MSI method is a low-cost system and with simple data, suited for real-time usage in food. In recent years, MSI technology has been reported to have significant potential in food safety area such as food quality and safety inspection in meat or meat products.[19-21] However, all the above-mentioned researches were within the range of 400-970nm of which most of them did not involve the quantitative analysis of pork eating quality.

The main aim of this work is to search a non-destructive, rapid, simple and low-cost method for sensing pork eating quality. Here, we developed a low-cost and simple MSI system from a complicated HSI system using data dimension reduction and selecting band-filters; besides, we systematically studied the efficient nonlinear algorithms for modeling. Accordingly, the specific objectives of the study include: selection of characteristic wavelengths using HSI; construction of MSI system and acquisition of multispectral images; preprocessing of multispectral images; extraction of characteristic parameters from region of interest (ROI); and the use of PLS, BP-ANN and ACO-BPANN algorithms for modeling, as well as testing the model using independent samples.

2. Materials and methods

2.1. Samples preparation

Samples (longissimus muscle) were purchased from fifteen pigs' carcasses in a local supermarket (Auchan, Xuefu road, Zhenjiang, China) and taken to the laboratory in 30 min. Pigs were slaughtered under commercial conditions (stunned electrically, exsanguinated, scalded, de-haired, eviscerated and split into sides), and no different treatments at slaughter were carried out. Test samples were chopped into 103 pieces of 6×3×3cm (length × width × thickness) on a sterile surface of the laboratory and the weight of each sample was about 80±0.5g. Before analysis, all samples were vacuum-packed with sealing plastic bags, labeled and stored in a refrigerator at 4ºC.

2.2. Characteristic wavelengths selection

First of all, the HSI system, shown in Fig.1a and developed by the Agricultural Product Processing and Storage Lab at Jiangsu University, was used for acquisition of pork hyperspectral images. The system mainly consists of a high performance back-illuminated CCD camera (V10EB1610, Spectral Imaging Ltd., Finland) with a spatial resolution of 320×256 pixels; a line-scan spectrograph (ImSpector V10E2/3", Spectral Imaging Ltd., Finland) with a nominal spectral resolution of 5.0nm; a 150 W quartz-halogen DC illuminator (Fiber-Lite PL900-A, Dolan-Jenner Industries Inc., USA); a linear motorized slide (Zolix SC30021A, Zolix. Corp., China); an enclosure; a data acquisition and pre-processing software; and a computer. The spectrograph collected spectral images in a wavelength range of 870-1770nm, with a spectral interval of 3.5156nm, which resulted in 256 spectral bands. Two fiber-optic light-guiding branches from the DC illuminator were mounted on the enclosure as light sources. The linear motorized slide was used to move the sample using a stepper motor controlled by the computer via a serial port so that both camera scanning and slide motion could be synchronized. A scanning rate was selected to achieve a square pixel. The whole imaging system was enclosed in a duralumin shield box (350×500×800 mm) to avoid the interference from external light.

The obtained hyperspectral data is a 3-D datacube including 256 images of the wavelength ranging from 870nm to 1770nm, while such huge data substantially increases computational burden. Additionally, the neighboring band pictures from hyperspectral image data are highly correlated. The band-to-band correlation creates redundant information in the hyperspectral image data.[22] Hence, it is necessary to extract optimum characteristic pictures from hyperspectral datacube that are related to pork quality. Principal component analysis (PCA) is one of the techniques commonly used for dimensionality reduction intending to eliminate redundant bands and diminish computational burden. The front PC images, which express most information of original data, were found according to their variance contribution. Each PC image is a linear sum of the original images at individual wavelengths multiplied by corresponding (spectral) weighting coefficients. Two or three bands with higher (local maximum) weighting coefficients from the optimum PC image are selected as the dominant bands. PCA was implemented in ENVI 4.5 (Research System, Inc., USA).

2.3. Multispectral imaging system and image acquisition

According to the dominant bands selected from hypercube, the study designed a multispectral imaging (MSI) system using the corresponding bandpass filters, which was developed by the Agricultural Product Processing and Storage Lab at Jiangsu University (see Fig.1b). The MSI system mainly consists of a charge-couple device (CCD) camera (XS-1828XC117B, Xenics infrared solution, Belgium) with spatial resolution of 320×256 pixels, three 150 W quartz-halogen DC illuminators (Fiber-Lite PL900-A, Dolan-Jenner Industries Inc., USA), a rotate wheel of filters, filters of characteristic bands (1280±10nm, 1440±10nm and 1660±10nm; Optical Insight, Inc., Santa Fe, NM), computer, and image processing and analysis software (Matlab R2009b; The Math-works, Natick, MA, USA). The whole imaging system was enclosed in a duralumin shield box (350×500×800mm) to avoid the interference from external light.

[Here for Fig. 1]

Prior to image acquisition, the multispectral imaging system was opened to preheat for 30 min. At the same time, the samples were taken out of the refrigerator and placed for 30 min at room temperature (25±1°C), and then they were placed on the conveying stage in multispectral imaging system for multispectral data acquisition.

2.4. References measurement

Warner-Bratzler Shear Force (WBSF) was one of reference methods in measurement of pork's tenderness, which was reported in many literatures.[1, 6, 23] In this experiment, the WBSF measurement in pork was performed according to Chinese standard NY/T 1180-2006. After images acquisition, samples were immediately vacuum-packed in nylon/polyethylene bags, and cooked in water bath at 80ºC until the internal temperature of pork reached 70ºC. WBSF was measured by the TA-XT2i (Stable Micro Systems Limited Co., England) equipped with one Warner-Bratzler shear blade (cross-head speed of 1 $mm \cdot s^{-1}$). Then, the sample was sheared perpendicular to the muscle fibres. WBSF was determined according to the peak in the force deformation curve, and its unit was kilogram force abbreviated as kgf. In this work, each sample was measured five times, and the average of the five measurement results was used for further analysis.

Water-holding capacity (WHC) is defined as the ability of muscle to retain water or resist water loss.[7] Various kinds of methods was used for detection of pork's WHC, such as centrifuge force method, cooking loss, tray drip loss method and EZ drip loss method.[9] In this experiment, the WHC measurement was performed according to the cook loss (CL). For the determination of CL, samples were vacuum-packed in nylon/polyethylene bags and cooked by immersion at 80ºC until the internal temperature of pork reached 70ºC in water bath. The pork samples were cooled to 25ºC. Next, the surface water of pork was wiped out with filter paper (Hangzhou Whatman-Xinhua Filter Paper Co.Ltd., Hangzhou, China). The difference of weight before and after cooking was used for calculation of CL.

2.5. MSI images preprocessing

2.5.1 ROI segmentation

Some information from original image is irrelevant to the analysis such as its surroundings. To ensure that this irrelevant information will not interfere with the analysis, a pre-processing step is needed. Each individual spectral band image was extracted separately through defining a region of interest (ROI). A quadrate ROI with a size of 50×50 pixels was selected by Matlab programs.

2.5.2 Extraction of texture feature variables

Gray level co-occurrence matrix (GLCM) has been widely used to extract image texture information.[4, 24] Each element (i, j) in GLCM represents the probability that two pixels with the gray level *i* and *j* co-occur in the image separated by a distance along a given direction (0°, 45°, 90°, and 135°). Theoretically, a variety of GLCM could be constructed from the image with different values of direction and distance. In this study, four textural features including contrast, correlation, energy, and homogeneity were extracted by GLCM texture analysis. Generally, contrast is used to express the local variations present in the image. Correlation is a measure of image linearity among pixels and the lower the values, the less the linear correlation. Energy that measures the textural uniformity of the image is the sum of squared elements in the GLCM. Finally, homogeneity usually measures the closeness of the distribution of elements in the GLCM to its diagonal. The above mentioned parameters were calculated at one distance (D = 1) for each pixels in the GLCM at each direction (0°, 45°, 90°, and 135°). The mean and standard deviation of each image were calculated. Then, the model prediction was conducted by Matlab programs using texture feature parameters (contrast, correlation, energy, and homogeneity under 4 directions, mean and standard deviation) from three characteristic pictures (totaling 54 variables for one sample) as the input variables whereas the measured values of WBSF and WHC as the output variables. The whole steps involved in building prediction models are depicted in the flowchart shown in Fig. 2.

[Here for Fig. 2]

2.6. Software

Hyperspectral imaging data was acquired by SpectralCube (ImSpector, image, Auto Vision Inc., USA). Characteristic wavelengths optimization was implemented in ENVI 4.5 (Research System, Inc., USA). Multispectral imaging data acquisition software was compiled based on Microsoft VC++ platform, and. All data algorithms were implemented in Matlab R2009b (Matworks Inc., Natick, MA, USA) in Windows 7.

3. Results and discussion

3.1. Calibration of models

All 103 samples were divided into two subsets. The first subset was called calibration set used to build a model, while the other one was called prediction set used to test the robustness of model. Selecting samples for modeling and the procedure was done as follows: first, all samples were sorted according to their respective *y*-value (viz. the reference values of WBSF and CL); then, one sample of every three samples was entered into the prediction set. Thus, the calibration set contained 69 samples, and the prediction set contained 34 samples. As shown in Table 1, the ranges of two reference values of WBSF and CL in the calibration set almost cover the range in the prediction set, and their standard deviations in the calibration and prediction sets have no significant differences. Therefore, their distributions of the samples are reasonable in the calibration and prediction sets.

3.2. Results of wavelengths optimization

In spectral range, according to the investigation of spectra of 870-1700nm, too much noise was exhibited in the spectral regions below 900nm and over 1700nm, and thus, the spectral region of 900-1700nm was selected. In this study, PCA was used to reduce the hyperspectral data dimension. PC1 image is shown in Fig. 3, which is the first PC image obtained by PCA. It is found that the first principal component (PC1) image is the best representation of original sample, because the variance contribution rate explained by PC1 image is the highest, reaching 95.53%. Thus, the dominant bands are determined according to PC1 image in this work, and four dominant bands (i.e. 976.759nm, 1281.865nm, 1436.192nm and 1662.201nm) with higher weight coefficients are selected by investigating all weighting coefficients. It is seen that the selected wavelengths for pork quality were closely related to the water and fat content of the samples. The absorption bands of 976.759nm, 1281.865nm, 1436.192nm and 1662.201nm are due to O-H bonds attributed to water content or C-H bonds related to fat content,[4] just as known, the main ingredients of meat are protein, fat, carbohydrates and water. Accordingly, the images at these 4 dominant bands can respond to the quality of pork. In order to make the system simple, the researchers choose three of the wavelengths to establish multispectral imaging system. Thus, the multispectral band pass filters with bandwidths of 1280±10nm, 1440±10nm and 1660±10nm were selected.

[Here for Fig. 3]

3.3. Results of ACO-BPANN models

As mentioned above, the change of pork quality is often accompanied with the changes from the external attributes (color, texture, etc.) and internal attributes (chemical compositions, tissue structure, etc.). The three images of multispectral data-cube can express the changes of external attributes of pork meat, and the spectral information can express the internal attributes changes. Thus, there exists indirect correlation between quality of pork meat and multispectral data. However, the feature variables, extracted from characteristic images, may have linear correlation. Moreover, the correlation information is redundant and unfavorable for establishment of simple model. In this work, MSI technique combined with variable selection method (Ant colony optimization (ACO)) was used to develop BP-ANN model for prediction of WBSF and CL in pork.

ACO [25] is an optimization method that can be used for feature selection. It resembles the behavior of ant colonies in the search for the best path to food sources without the use of visual information, which employs the concept of cooperative pheromone accumulation, and optimizes models using a pre-defined number of variables, occupying a Monte Carlo approach to discard irrelevant variables.[26] It has an advantage over simulated annealing and genetic algorithm approaches of similar problems where the graph may change dynamically; the ant colony algorithm can be run continuously and adapt to changes in real-time.[27] Presently, ACO shows its high potential in discarding irrelevant information regions, and has been widely used for characteristic variable selection.[28] In this work, the required parameters for running ACO algorithm were set as follows according to experience based on substantial trials: the initial population was set to 80; the maximum number of iterations was set to 50; the maximum number of cycles was set to 20; the probability threshold of variable selection was set to 0.3; and the pheromone attenuation coefficient was set to 0.65.

For the HSI data processing, there are many algorithms have been reported in many published literatures, such as, PLS, SVM, ANN.[16, 29] BP-ANN is a strong tool for capturing and revealing complex relationship between inputs and outputs. BP-ANN is the commonly used feed-forward multilayer networks.[30, 31] It consists of neurons arranged in layers (an input layer, one or more hidden layers and an output layer) being the connections (weights) unidirectional from input to output.[31-33] The optimal model was determined by the lowest root mean square error of cross validation (*RMSECV*). Other parameters of the BP-ANN model were optimized by the minimal mean square error (*MSE*). Herein, the number of neurons in the hidden layer was set as 5, the learning rate factor and momentum factor were set as 0.1, the initial weight was set as 0.3 and the scale function was set as 'tangential hyperbolic (tanh)' function.

Fig. 4a presents the textural features variables selected by ACO algorithm, which containing a total of 10 variables. It indicated that these 10 variables were highly correlated with WBSF of pork. Fig. 4b is the scatter plot between reference measurements of WBSF and MSI predicted results in the calibration and prediction sets. Here, the value of RMSECV is 0.921kgf and correlation coefficient (Rc) is 0.9267 in calibration set, when the performance of BP-ANN model is evaluated by the samples in the prediction set, the value of RMSEP is 0.9087kgf and correlation coefficient (Rp) is 0.8451. Fig. 4c presents the textural features variables selected by ACO algorithm, which containing a total of 14 variables. It indicated that these 14 variables were highly correlated with CL of pork. Fig. 4d is the scatter plot between reference measurements of CL and MSI predicted results in the calibration and prediction sets. Here, the value of RMSECV is 1.3391% and correlation coefficient (Rc) is 0.9533 in calibration set; when the performance of BP-ANN model is evaluated by the samples in the prediction set, the value of RMSEP is 1.5129% and correlation coefficient (Rp) is 0.9116.

[Here for Fig. 4]

3.4. Discussion of the results

In order to highlight the superiority of ACO-BPANN algorithm, the classical partial least squares (PLS) and BP-ANN were studied systematically and comparatively in this work. All the results are shown in Table 2. Investigated from this table, all the regression models showed good performances, which further verified that it is feasible and reliable to analyze WBSF and CL of pork meat quantitatively with the selected wavelengths using the developed multispectral imaging system. Moreover, the results of BP-ANN models are much better than that of PLS models. In addition, in the case of the two parameters, the regression models made great progress after ACO variables selection. Results revealed that ACO-BPANN is extremely suitable for determination of pork's WBSF and CL by MSI technique.

The reasons for results could be explained as follows. Firstly, it might be explained by the histological basis of pork. Muscle tissue is composed of myofibrils, and each of the myofibril consists of myosin heavy-chain and actin filaments. Differences in μ-calpain, m-calpain, and calpastatin activity may ultimately influence the tenderness and water-holding capacity of pork by impacting the rate of myofibril, adipose tissue and water.[34-36] Furthermore, after cooking, the adipose tissue cells rupture and the intramuscular fat redistributes, which also affect the pork eating quality. The distribution of myofibrils, adipose tissue and water forms the texture which can be captured by MSI data, thus, the MSI images can indirectly reflect the pork quality. Therefore, all the models achieved good performances, indicating that it is feasible and reliable to estimate WBSF and CL quantitatively using our developed MSI system.

Secondly, BP-ANN model was compared with PLS model. Compared to the linear regression tool i.e. PLS, BP-ANN is a universal nonlinear regression tool which has stronger robustness, self-learning and adaptation than linear method. When faced with complex problems, nonlinear method might be more suitable for the solution of data prediction.[12, 37] In contrast with the linear structure of PLS, the topological network architecture of BP-ANN may be more suitable for the analysis of complicated measurement.[38] In fact, the relationships between the WBSF/CL and the multispectral data were diagnosed by the approach of augmented partial residual plots (APARPs).[39] A quantitative numerical tool (run test) was employed to calculate the non-linearity based on APARPs method; the $|z|$-value is 8.912 for WBSF, and 8.512 for the CL, respectively; both of them exceed the critical value ($|z| = 1.96$). The results were shown in Table 3. Therefore, it can be concluded that there is a non-linear relationship between multispectral images and WBSF/CL, and the linear tools might not be able to provide a complete solution to so complicated regression.

Thirdly, ACO-BPANN model was compared with BP-ANN model. The absorption bands at characteristic wavelengths of 1280nm, 1440nm and 1660nm are due to O-H bonds related to water content.[5, 14, 40] Therefore, the texture feature variables, which were extracted from 3 MSI images, may have linear correlation. Moreover, like ants finding food, ACO algorithm is good for optimization of variables. The variables optimized by ACO which were closely related to pork quality, were used as the input of model. Thus, compared with BP-ANN model and PLS model, ACO-BPANN model has a best result.

4. Conclusions

This work shows the potential of near infrared MSI technique in determination of WBSF and WHC in pork are the two important parameters of pork's eating quality. In developing prediction models, ACO-BPANN revealed its superiority in contrast to classical PLS and BP-ANN calibration methods. It can be concluded that the MSI system with efficient algorithm would achieve the promotion of emerging imaging technique from the laboratory research to the practical usage for real-time monitoring meat quality.

Acknowledgment

This work has been financially supported by the National Natural Science Foundation of China (31371770). We are also grateful to many of our colleagues for stimulating discussion in this field.

References

1. J. Cai, Q. Chen, X. Wan and J. Zhao, *Food Chemistry*, 2011, **126**, 1354-1360.
2. B. Leroy, S. Lambotte, O. Dotreppe, H. Lecocq, L. Istasse and A. Clinquart, *Meat Science*, 2004, **66**, 45-54.
3. F. Tao, Y. Peng, Y. Li, K. Chao and S. Dhakal, *Meat Science*, 2012, **90**, 851-857.
4. M. Kamruzzaman, G. ElMasry, D.-W. Sun and P. Allen, *Analytica Chimica Acta*, 2012, **714**, 57-67.
5. M. Kamruzzaman, G. ElMasry, D.-W. Sun and P. Allen, *Food Chemistry*, 2013, **141**, 389-396.
6. Y. L. Xiong, M. J. Gower, C. Li, C. A. Elmore, G. L. Cromwell and M. D. Lindemann, *Meat Science*, 2006, **73**, 600-604.
7. D. Tejerina, S. García-Torres and R. Cava, *Livestock Science*, 2012, **148**, 46-51.
8. D. K. Pedersen, S. Morel, H. J. Andersen and S. Balling Engelsen, *Meat Science*, 2003, **65**, 581-592.
9. M. Prevolnik, M. Čandek-Potokar and D. Škorjanc, *Journal of Food Engineering*, 2010, **98**, 347-352.
10. S. M. Fowler, H. Schmidt, R. van de Ven, P. Wynn and D. L. Hopkins, *Meat Science*, 2014, **98**, 652-656.
11. Q. Chen, J. Cai, X. Wan and J. Zhao, *LWT - Food Science and Technology*, 2011, **44**, 2053-2058.
12. Q. Chen, Z. Hui, J. Zhao and Q. Ouyang, *LWT - Food Science and Technology*, 2014, **57**, 502-507.
13. G. K. Naganathan, L. M. Grimes, J. Subbiah, C. R. Calkins, A. Samal and G. E. Meyer, *Computers and Electronics in Agriculture*, 2008, **64**, 225-233.
14. G. ElMasry, D.-W. Sun and P. Allen, *Journal of Food Engineering*, 2012, **110**, 127-140.
15. K. Cluff, G. Konda Naganathan, J. Subbiah, A. Samal and C. R. Calkins, *Meat Science*, 2013, **95**, 42-50.
16. D. Wu and D.-W. Sun, *Talanta*, 2013, **116**, 266-276.
17. H. Li, Q. Chen, J. Zhao and M. Wu, *LWT - Food Science and Technology*, 2015, **63**, 268-274.
18. Q. Chen, C. Zhang, J. Zhao and Q. Ouyang, *TrAC Trends in Analytical Chemistry*, 2013, **52**, 261-274.
19. X. Sun, K. J. Chen, K. R. Maddock-Carlin, V. L. Anderson, A. N. Lepper, C. A. Schwartz, W. L. Keller, B. R. Ilse, J. D. Magolski and E. P. Berg, *Meat Science*, 2012, **92**, 386-393.
20. F. Ma, J. Yao, T. Xie, C. Liu, W. Chen, C. Chen and L. Zheng, *Food Research International*, 2014, **62**, 902-908.
21. E. Z. Panagou, O. Papadopoulou, J. M. Carstensen and G.-J. E. Nychas, *International Journal of Food Microbiology*, 2014, **174**, 1-11.
22. L. Huang, J. Zhao, Q. Chen and Y. Zhang, *Food Research International*, 2013, **54**, 821-828.
23. J. Wu, Y. Peng, Y. Li, W. Wang, J. Chen and S. Dhakal, *Journal of Food Engineering*, 2012, **109**, 267-273.
24. G. ElMasry, N. Wang, A. ElSayed and M. Ngadi, *Journal of Food Engineering*, 2007, **81**, 98-107.
25. M. Dorigo and L. M. Gambardella, *Evolutionary Computation, IEEE Transactions on*, 1997, **1**, 53-66.
26. F. Allegrini and A. C. Olivieri, *Analytica Chimica Acta*, 2011, **699**, 18-25.
27. V. S. D. R. Umarani and V. Selvi, *International Journal of Computer Applications (0975–8887) Volume*, 1-6.
28. X. W. Huang, X. B. Zou, J. W. Zhao, J. Y. Shi, X. L. Zhang and M. Holmes, *Food Chemistry*, 2014, **164**, 536-543.
29. H.-J. He and D.-W. Sun, *Trends in Food Science & Technology*, 2015, **46**, 99-109.
30. F. Ahmed, *Molecular Cancer*, 2005, **4**, 29.
31. L. Yu, S. Wang and K. K. Lai, *Computers & Operations Research*, 2005, **32**, 2523-2541.
32. K. Cai, J. Xia, L. Li and Z. Gui, *Computational Materials Science*, 2005, **34**, 166-172.
33. T.-L. Lee, *Ocean Engineering*, 2004, **31**, 225-238.
34. A. H. Karlsson, R. E. Klont and X. Fernandez, *Livestock Production Science*, 1999, **60**, 255-269.
35. J. L. Melody, S. M. Lonergan, L. J. Rowe, T. W. Huiatt, M. S. Mayes and E. Huff-Lonergan, *Journal of Animal Science*, 2004, **82**, 1195-1205.
36. J. M. Hughes, S. K. Oiseth, P. P. Purslow and R. D. Warner, *Meat Science*, 2014, **98**, 520-532.

37. Q. Chen, Z. Guo, J. Zhao and Q. Ouyang, *Comparisons of different regressions tools in measurement of antioxidant activity in green tea using near infrared spectroscopy*, 2011.
38. H. Lin, Q. Chen, J. Zhao and P. Zhou, *Journal of Pharmaceutical and Biomedical Analysis*, 2009, **50**, 803-808.
39. V. Centner, O. E. de Noord and D. L. Massart, *Analytica Chimica Acta*, 1998, **376**, 153-168.
40. A. Iqbal, D.-W. Sun and P. Allen, *Journal of Food Engineering*, 2013, **117**, 42-51.

Figure captions

Fig.1. Near infrared spectral imaging system

Fig.2. Flowchart of predicting WBSF and CL in pork by MSI system

Fig.3. Dominant wavelengths selected by PCA

Fig.4. Results of ACO-BPANN models: (a) Variables selected by ACO algorithm for WBSF; (b) scatter plot between reference measurement of WBSF and ACO-BPANN predicted results; (c) Variables selected by ACO algorithm for CL; (d) scatter plot between reference measurement of CL and ACO-BPANN predicted results

Table 1 Reference measurement of WBSF and CL in the calibration and prediction sets.

Quality parameters	Units	Subsets	Sample number	Range	Mean	Standard deviation
WBSF	kgf	Calibration set	69	4.4678~9.8537	6.8921	1.2392
		Prediction set	34	5.0626~10.1651	6.9992	1.0182
CL	%	Calibration set	69	21.33~29.69	26.94	1.87
		Prediction set	34	22.09~30.7	27.04	1.74

Table 2 Calibration models for prediction of pork WBSF and CL using different algorithms

Quality parameters	Model	Variables	Prediction set Rp
WBSF	PLS	54	0.7481
	BP-ANN	54	0.8253
	ACO-BPANN	10	0.8451
CL	PLS	54	0.7786
	BP-ANN	54	0.8876
	ACO-BPANN	14	0.9116

Table 3 Results of the runs test used for the detection of the linearity relationship between the MSI data and the WBSF and CL based on APaRPs method

Quality parameters	n_+	n_-	u	μ	σ	|z|	Result
WBSF	52	51	7	52.5	5.05	8.91	Nonlinear
CL	54	49	9	52.4	5.04	8.51	Nonlinear

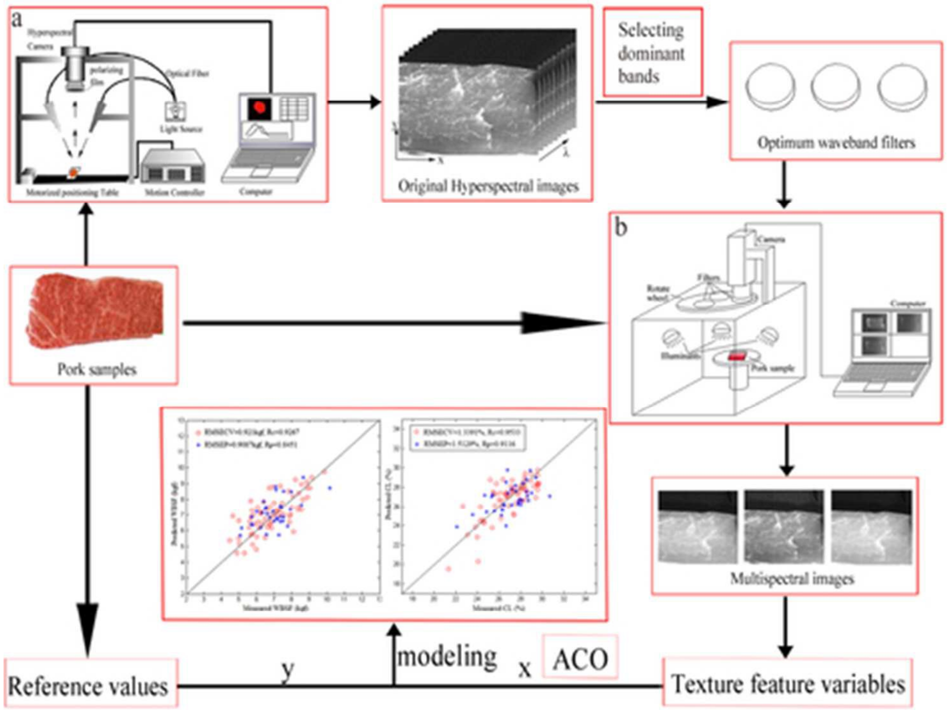

39x30mm (300 x 300 DPI)

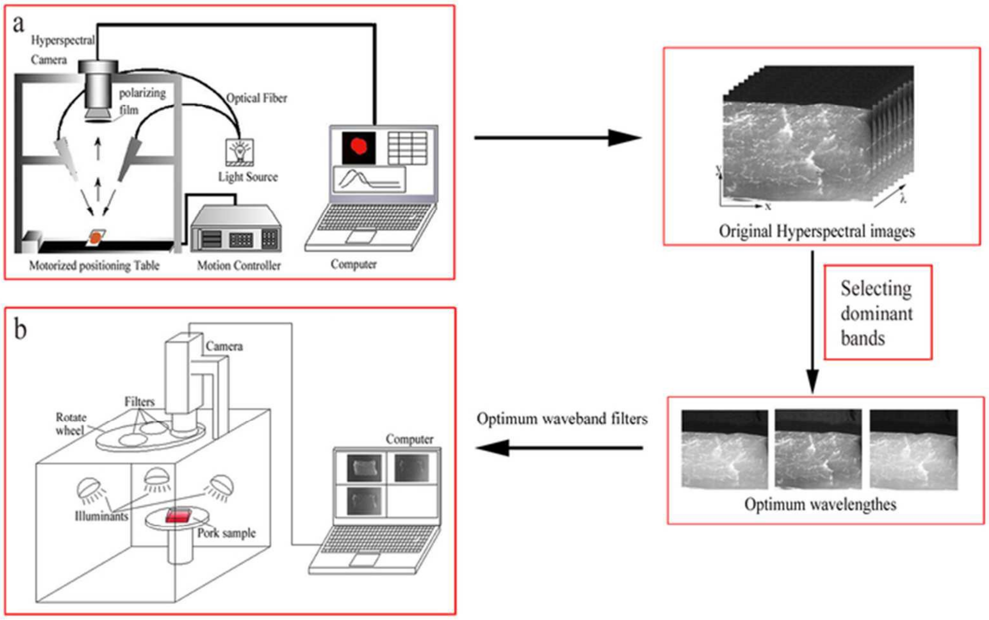

63x39mm (300 x 300 DPI)

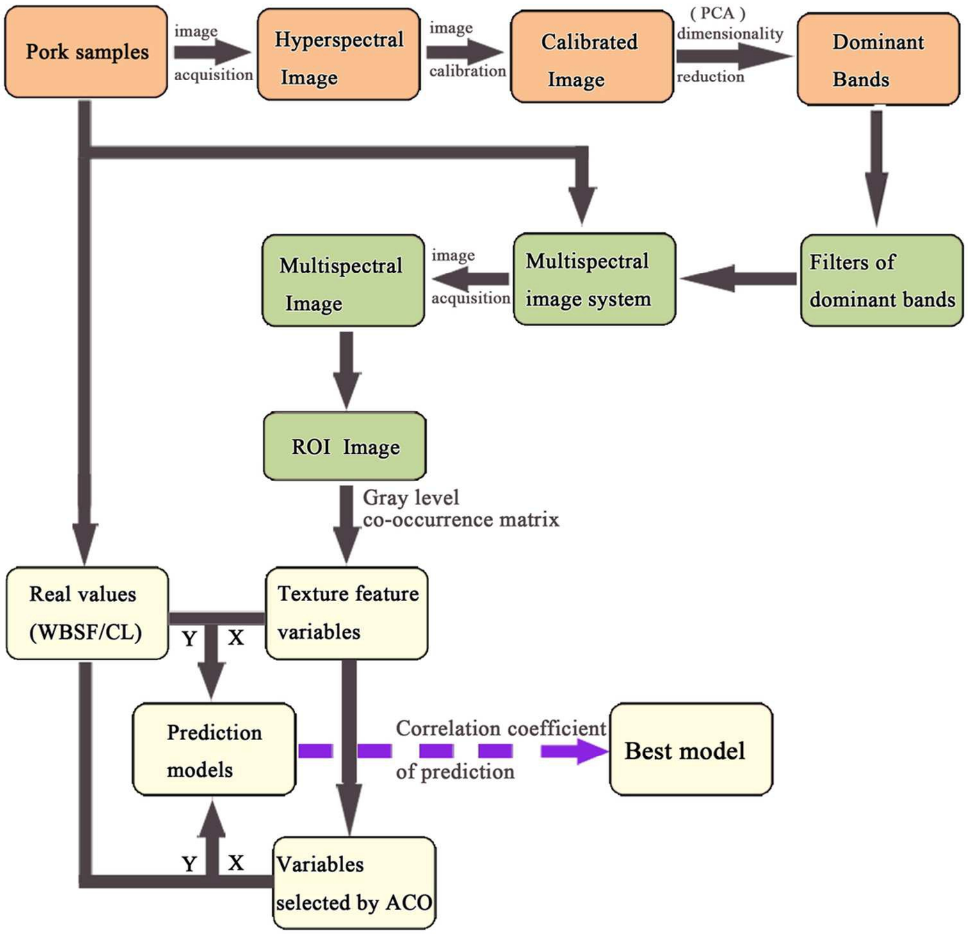

96x93mm (300 x 300 DPI)

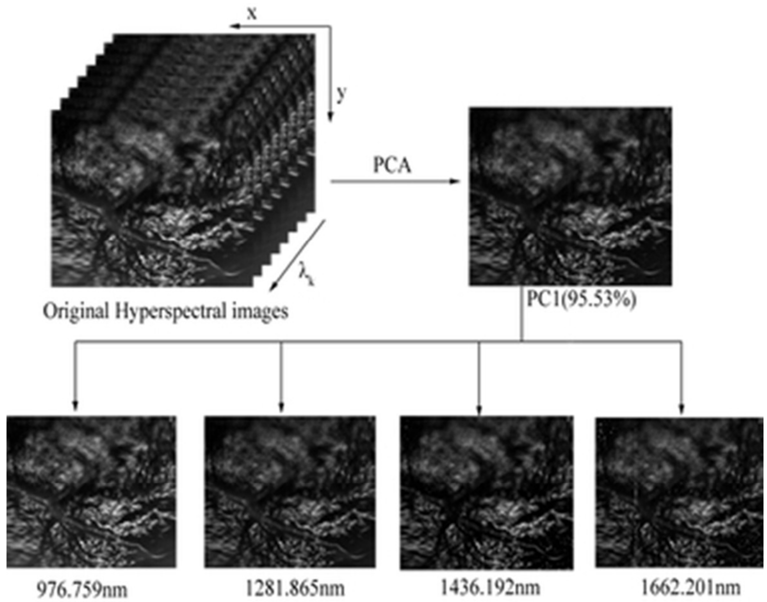

32x25mm (300 x 300 DPI)

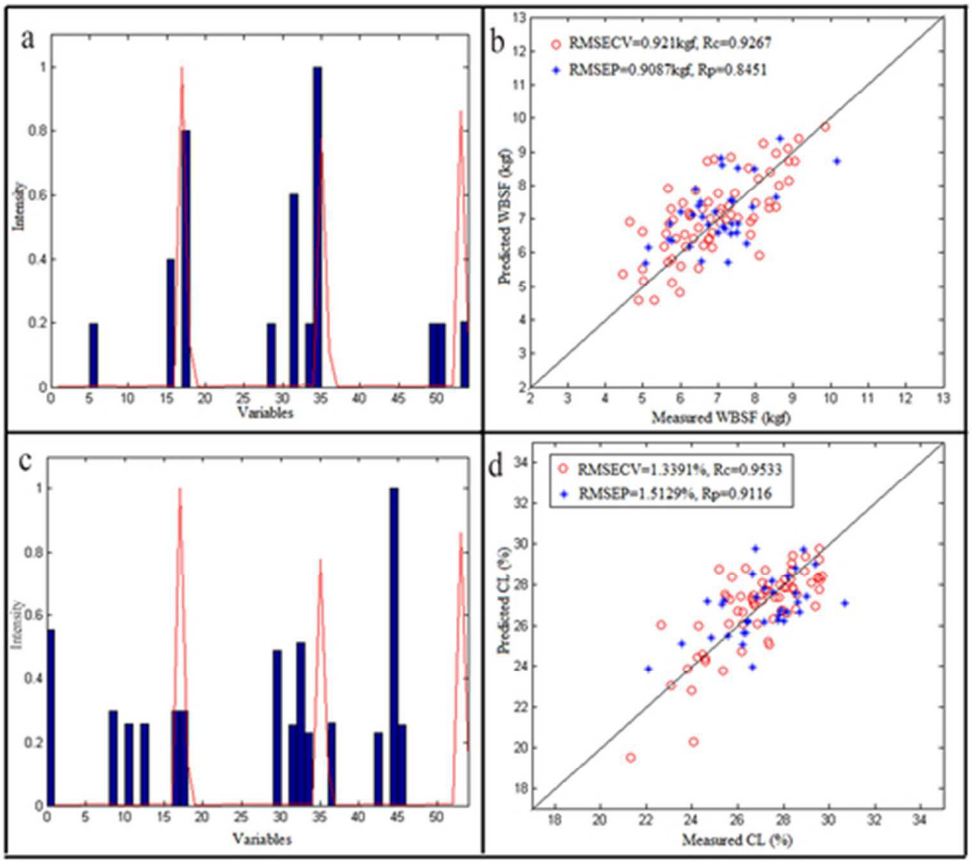

43x37mm (300 x 300 DPI)